A new family of biocompatible and stable magnetic nanoparticles: silica cross-linked pluronic F127 micelles loaded with iron oxides

Zhaoyang Liu,* Jun Ding and Junmin Xue*

Received (in Montpellier, France) 18th June 2008, Accepted 4th September 2008
First published as an Advance Article on the web 15th October 2008
DOI: 10.1039/b810302j

A new family of magnetic nanoparticles, silica cross-linked pluronic F127 micelles loaded with iron oxides having the properties of high biocompatibility, physical and chemical stability, high magnetism, and low-cost production, have been synthesized.

1. Introduction

Iron oxide (IO) nanoparticles are emerging as promising candidates for various biomedical applications, such as magnetic resonance imaging (MRI),[1] targeted drug delivery,[2] hyperthermia treatment,[3] the labelling and sorting of cells,[4] and the separation of biochemical products,[5] due to their superparamagnetic properties. Most of these applications require the nanoparticles to be biocompatible, water soluble, and physically and chemically stable in a physiological environment.[6] To date, the most promising synthetic strategy for iron oxide nanoparticles is based on the high temperature decomposition of iron salts in the presence of organic solvents, which can produce monodisperse and highly crystalline IO nanoparticles.[7] However, their uses in biomedicine are quite limited because the particles synthesized through this route can only be dispersed in hydrophobic solvents. Before biomedical applications are possible, they have to be transferred into an aqueous medium. Moreover, the reactivity of iron oxide particles have been shown to greatly increase as their dimensions are reduced to the nano scale. Therefore, it is necessary to engineer the surface of IO nanoparticles to improve their biocompatibility, solubility and stability in physiological environments for various biomedical applications.[8]

Several natural and synthetic polymers have been employed to coat the surface of IO nanoparticles to transfer their surface wettability. These polymers include dextran,[9] lipids,[10] dendrimers,[11] polyethylene glycol (PEG)[12] or polyethylene oxide (PEO),[13] and polyvinylpyrrolidone (PVP).[14] All the polymers used are known to be biocompatible and able to promote the dispersion of IO nanoparticles in an aqueous medium. However, these polymer coatings are not robust and can be detached from particle surfaces easily under *in vivo* conditions.[10,12] To improve the stability of the polymer coatings *in vivo*, a cross-linking technique has been developed.[15] For example, the stability of dextran coatings on IO nanoparticles can be improved when the dextran polymer chains are chemically cross-linked. Although cross-linking is considered a promising method for strengthening the polymer coatings of IO nanoparticles,[16–19] this method requires multiple synthetic steps (multi-pot).[18] Therefore, a simple and one-pot method is in demand.

In this work, we have developed a simple and one-pot method to fabricate a new family of biocompatible and stable magnetic nanoparticles that are coated with a hybrid layer of silica cross-linked pluronic F127 (SCL-P@IO). Pluronic F127 (PF127) is an ABA-type triblock copolymer consisting of hydrophobic poly(propylene oxide) (PPO) and hydrophilic PEO. The PEO blocks present a high biocompatiblity by effectively preventing aggregation, the adsorption of proteins, the adhesion to tissues, and recognition by the reticuloendothelial system *in vivo*.[20] Silica has been extensively studied as an inorganic coating for a long period of time due to its rich surface chemistry, which means it is able to conjugate biofunctional moieties easily. Compared to polymer coatings, silica coatings are more chemically stable and resistant to diffusion for encapsulated components. PF127 copolymer and silica have also been selected as suitable surface coating candidates because they are highly safe *in vivo* and have been approved by the Food and Drug Administration.[20,21]

A double-layer coating of PEO and silica on the surface of IO nanoparticles is proposed, as shown in Fig. 1a. Like conventional mesoporous silica synthesis using PF127 surfactants,[22] the silica was controlled so as to be deposited on the interior PEO blocks of the PF127 micelle, leaving the exterior PEO blocks stretched out in aqueous media. Therefore, a double-layer structure of PEO and silica on the surfaces of the IO nanoparticles was formed (Fig. 1a). The advantages of the resulting magnetic nanoparticles are follows: (1) high biocompatibility and stability due to the presence of PEO blocks on the surface of the nanoparticles, (2) high chemical and physical stability due to the robust and dense silica cross-linked micelles, and (3) simple and low-cost synthesis, since silica cross-linking is much easier in comparison with traditional polymer cross-linking, and since both PF127 and the silica precursor are commercially available. Therefore, the present magnetic nanoparticles possess great potential in a variety of biomedical applications.

2. Experimental

2.1 Materials

Dioctyl ether, oleic acid, iron(III) chloride, tetraethoxysilane (TEOS), diethoxydimethylsilane ($Me_2Si(OEt)_2$, DEDMS) and

Department of Materials Science and Engineering, National University of Singapore, Singapore, 117576, Republic of Singapore. E-mail: mselz@nus.edu.sg. E-mail: msexuejm@nus.edu.sg; Fax: +65 67763604; Tel: +65 65164655

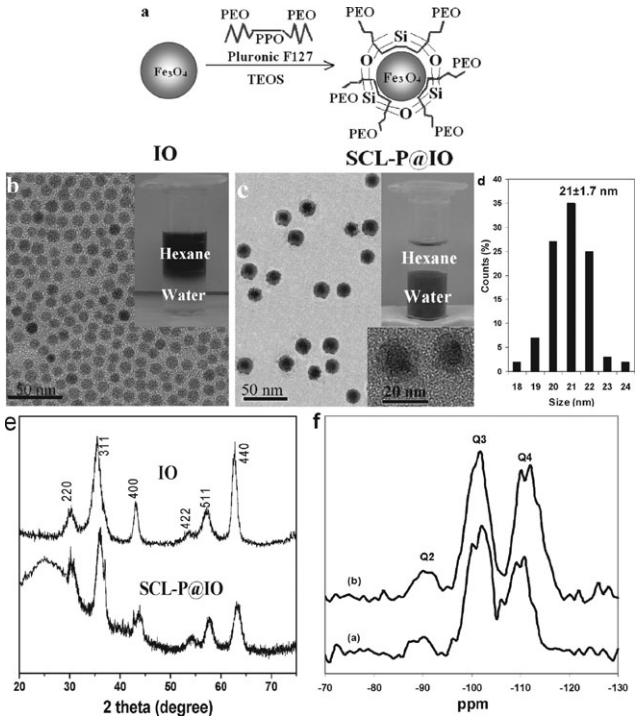

Fig. 1 **a**: Synthetic scheme for silica cross-linked pluronic F127 micelles loaded with IO nanoparticles (SCL-P@IO). Left: an as-synthesized hydrophobic IO nanoparticle. Right: an IO nanoparticle with its surface covered by a double-layer of PEO and silica. **b**: A TEM of as-synthesized hydrophobic IO nanoparticles. The inset photo shows that the IO nanoparticles can only be dispersed in hexane. **c**: A TEM of SCL-P@IO nanoparticles. The right bottom inset is a higher magnification TEM of typical SCL-P@IO nanoparticles. The inset photo shows that the SCL-P@IO nanoparticles can be readily dispersed in water. **d**: Size distribution histogram of the nanoparticles in **c**. **e**: XRD patterns of IO and SCL-P@IO nanoparticles. **f**: ^{29}Si NMR spectra corresponding to samples (a) with and (b) without the addition of DEDMS, respectively.

pluronic F127 (PF127) were purchased from Aldrich Chemical Co. Fibroblasts 3T3 were purchased from ATCC. RPMI-1640 medium, Dulbecco's modified Eagle's medium (DMEM), fetal bovine serum (FBS), L-glutamine, penicillin and streptomycin were purchased from Sigma. All other solvents and chemicals were purchased from Aldrich and used as received.

2.2 Synthesis of IO nanoparticles (Fe_3O_4)

$FeCl_3{\cdot}6H_2O$ (3.3 mmol) and sodium oleate (10 mmol) were dissolved in a mixture of ethanol (25 mL), de-ionized water (20 mL) and hexane (45 mL). After refluxing for 4 h at 62 °C, the iron oleate complex was washed with de-ionized water three times. The iron oleate complex (3.3 mmol) and oleic acid (1.67 mmol) were dissolved in dioctyl ether (20 mL) at 70 °C. After heating for 1.5 h at 290 °C, ethanol (30 mL) was added to the mixture, and the nanoparticles were collected by centrifugation at 6000 rpm. The nanoparticles were washed with hexane and ethanol three times. Finally, the nanoparticles were dispersed in hexane (40 mL) and oleic acid (100 μl).

2.3 Synthesis of SCL-P@IO nanoparticles

A hexane solution (0.2 mL) of IO nanoparticles was added to an aqueous solution (8 mL) of PF127 (1.3 g). After 3 h of stirring at room temperature, the mixture was dried under nitrogen gas. The obtained powder could be readily redispersed in de-ionized water (8 mL) with shaking. Then, a 0.3 M HCl solution (0.4 g) and TEOS (0.2 g) were added to the mixture with stirring. After stirring at room temperature for 48 h, DEDMS (0.1 g) was added. Stirring was continued for another 3 h.

2.4 Cell culture

The cell viability of the nanoparticles was carried out by testing the viability of 3T3 fibroblasts after incubation with DMEM, supplemented with 10% FBS, 1 mM L-glutamine and 100 IU mL^{-1} penicillin *via* an 3-(4,5-dimethylthiazol-2-yl)-2,5-diphenyl tetrazolium bromide (MTT) assay. Mouse macrophage cells (RAW 264.7) were used to assess the cellular uptake of the nanoparticles. The RAW 264.7 cells were cultured in RPMI-1640 medium, supplemented with 10% FBS, 2 mM L-glutamine, 100 IU mL^{-1} penicillin and 100 mg mL^{-1} streptomycin. The cell concentrations were determined by hemacytometry, and the Fe concentrations were determined by Thermal Jarrell Ash Duo Iris inductively-coupled plasma optical emission spectrometer (ICP-OES).

2.5 Characterization

TEM measurements were taken using a JEOL JEM 3010 instrument. The hydrodynamic diameters of the nanoparticles were measured by a Malvern Zeta Sizer Nano S-90 dynamic light scattering (DLS) instrument. TGA analyses were performed by a TA Instruments Q500 thermogravimetric analyzer. IR studies were run on an ATI Mattson Infinity Series FT-IR spectrophotometer. Magnetic properties were measured on a superconducting quantum interference device (SQUID, Quantum Design, USA) and a Lakeshore 7300 series vibrating sample magnetometer (VSM). The fluorescence emission spectra of pyrene were measured by a fluorescence photometer (FP-777 Jasco) at 254 nm excitation. ^{29}Si NMR spectra were recorded with an Advance 500 Bruker spectrometer at 99.36 MHz. The pulse length was 6 μs (theta = π/6) with 6 s repetitions.

3. Results and discussion

3.1 TEM, XRD and ^{29}Si NMR

In a typical synthesis, 10.5 nm monodisperse and hydrophobic Fe_3O_4 nanoparticles were synthesized separately (Fig. 1b).[23] The as-synthesized Fe_3O_4 nanoparticles were coated with a layer of oleic acid, which made them only soluble in hydrophobic solvents (Fig. 1b inset photo). With the addition of PF127 surfactants, these polymeric surfactants self-assembled into a micellar structure, encapsulating the IO nanoparticles in their cores. The hydrophobic PPO block in the middle of the PF127 associated with the alkyl tail of the oleic acid through a hydrophobic interaction, while the two hydrophilic PEO blocks stretched out in aqueous media (Fig. 1a). Then, TEOS

was added as a silica precursor to polymerize and cross-link the PF127 micellar shells.

Fig. 1c shows a TEM image of the SCL-P@IO nanoparticles. The formation of well-defined core/shell morphologies is readily confirmed, since the Fe_3O_4 within the micelle cores is more electron-dense than the silica/PF127 hybrid shell. A higher magnification TEM of typical SCL-P@IO nanoparticles is shown in the right bottom of Fig. 1c. These nanoparticles have a number-average diameter of around 21 nm, as shown in the histogram in Fig. 1d, with an ultrathin (about 5 nm) silica shell deposited outside the Fe_3O_4 nanoparticles. A size distribution analysis, as shown in the histogram in Fig. 2a, reveals that the spherical NPs are monodisperse and have an average size of 7.9 ± 1.5 nm. The inset photo shows that the resulting nanoparticles can be readily dispersed in water. The XRD patterns of the IO and SCL-P@IO nanoparticles (Fig. 1e) can be assigned to the (220), (311), (400), (422), (511) and (440) reflections of the spinel structure of magnetite (JCPDS no. 19-0629). The broad band at 20–30° is due to the presence of amorphous silica, while the labelled peaks are associated with Fe_3O_4 nanocrystals.

The condensation of silicate during the preparation was studied by NMR techniques. Fig. 1f (a) and (b) correspond to the sample with and without the addition of DEDMS, respectively. In the ^{29}Si NMR spectra, three peaks at *ca.* −94, −104 and −114 ppm are assigned to Q2, Q3 and Q4 species with progressively increasing cross-linking (condensation).[24] After automatic calculation of the integrated area, the Q4 : Q3 ratio decreased from 0.91 (b) to 0.83 (a), indicating a slightly lower condensation of silicate with the addition of DEDMS.

3.2 DLS and FT-IR

The obtained SCL-P@IO nanoparticles were characterized by DLS. The DLS measurements of the IO and SCL-P@IO nanoparticles are shown in Fig. 2a. The hydrodynamic diameter of the SCL-P@IO nanoparticles is 43.3 nm, which is larger than that measured by TEM in Fig. 1c. This is because the light scattering measurement includes the PEO chains stretching out into the aqueous solution, which cannot be observed by TEM due to the low contrast of the PEO polymers.[25] This result also confirms the double-layer structure of PEO and silica on the surface of SCL-P@IO nanoparticles instead of just a single layer of silica; that is, the silica is deposited on the interior PEO chains, while the exterior PEO chains are stretched out into the aqueous solution, as suggested in Fig. 1a. The surface coating of the SCL-P@IO nanoparticles was further studied by IR analysis. As shown in Fig. 2b, silica formation is confirmed, since a band at 1080 cm^{-1}, assigned to Si–O–Si, is observed for these SCL-P@IO nanoparticles.[26] After calcination at 700 °C, the characteristic band of C–H at 1726 cm^{-1} disappears completely, while the band assigned to thermally stable silica is still observed.

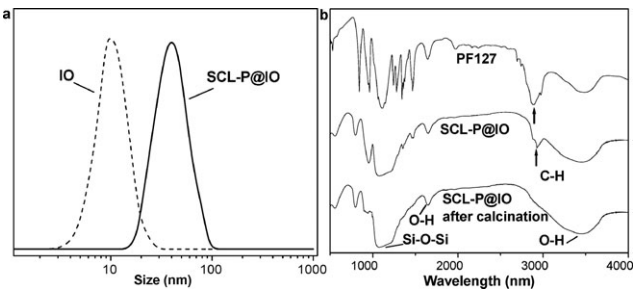

Fig. 2 a: Hydrodynamic sizes of IO and SCL-P@IO nanoparticles in aqueous solution determined by DLS measurements. b: IR spectra of PF127 triblock copolymer (top), SCL-P@IO nanoparticles (middle) and SCL-P@IO nanoparticles after calcination at 700 °C (bottom). The IR spectra of the SCL-P@IO nanoparticles are characteristic of both the silica network (Si–O–Si stretch at 1080 cm^{-1}) and the copolymer (C–H stretch at 1730 cm^{-1}). This C–H band disappears after calcination.

3.3 Magnetism characterization

The magnetic properties of the IO and SCL-P@IO nanoparticles were examined at room temperature by using a VSM. As shown in Fig. 3a, the saturated magnetization of the IO and SCL-P@IO nanoparticles were 63.1 and 28.3 emu g^{-1}, respectively. The reduction in saturated magnetization for the SCL-P@IO nanoparticles accounts for the diamagnetic properties of the silica and the PF127 shell surrounding the IO cores. The inset photo in Fig. 3a shows the magnetic manipulation ability of the SCL-P@IO nanoparticles. When an external magnet is placed beside the glass vial, the aqueous dispersion of SCL-P@IO nanoparticles could be directed towards the magnet. This efficient magnetism will allow these nanoparticles to be useful in many biomedical applications, such as targeted delivery and separation. The magnetization change of the SCL-P@IO nanoparticles with storage time was monitored by VSM measurements. As shown in Fig. 3b, the saturated magnetization of the SCL-P@IO nanoparticles was almost constant (at around 28 emu g^{-1}) during 90 d storage, suggesting that the PF127/silica hybrid coating is dense enough to be non-permeable, preventing the encapsulated IO cores from degrading and leading to lower magnetism.

3.4 Cell viability and uptake

The biocompatibility of the SCL-P@IO nanoparticles was examined by the cell viability of 3T3 fibroblast lines through

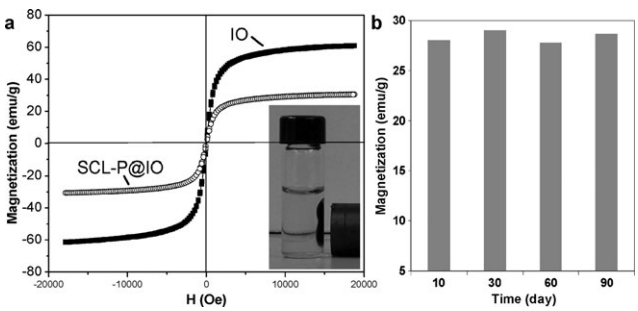

Fig. 3 a: Magnetization curves (*M*–*H*) of IO and SCL-P@IO nanoparticles. The inset photo shows that the SCL-P@IO nanoparticles can be driven by an external magnet. b: The magnetization change of the SCL-P@IO nanoparticles with storage time, as observed by VSM measurements.

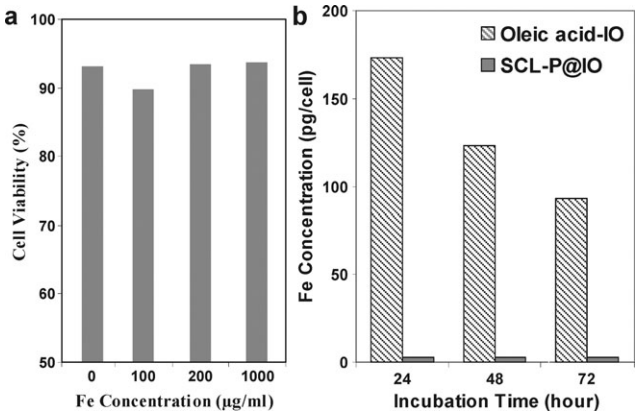

Fig. 4 a: Cell viability of 3T3 fibroblast lines after 72 h incubation with SCL-P@IO nanoparticles at different Fe concentrations. b: A macrophage uptake assay of oleic acid-stabilized nanoparticles (Oleic acid-IO) and SCL-P@IO nanoparticles with incubation time.

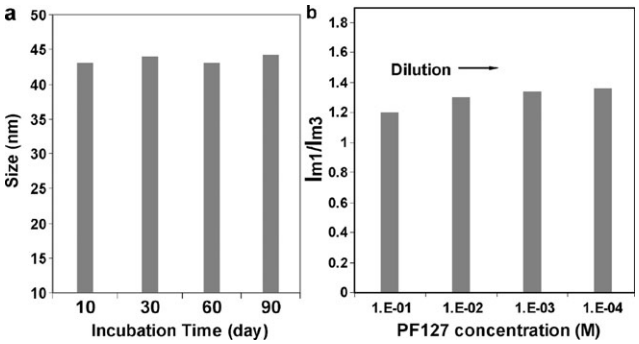

Fig. 5 (a) Hydrodynamic size changes of SCL-P@IO nanoparticles with incubation time in PBS buffer solution plus 10% FBS. (b) The fluorescence intensity ratio, I_{m1}/I_{m3}, of pyrene encapsulated in SCL-P@IO nanoparticles as a function of PF127 concentration. The I_{m1}/I_{m3} ratio for SCL-P@IO nanoparticles shows no obvious alteration, meaning the silica cross-linked micellar structure is stable under dilution.

an MTT assay. As shown in Fig. 4a, the SCL-P@IO nanoparticles were biologically inert up to an iron concentration of 1000 μg mL^{-1}. This result indicates that the SCL-P@IO nanoparticles are highly non-toxic and biocompatible. When injected into the bloodstream, nanoparticles are often considered as an intruder by the innate immunity system, and can be readily recognized and become engulfed by the macrophage cells. The nanoparticles will then be removed from the blood circulation system, and lose their efficiency in diagnostics and therapeutics.

Fig. 4b shows the uptake of the oleic acid-stabilized (Oleic acid-IO) and PEO-stabilized (SCL-P@IO) nanoparticles by macrophage cells with an initial Fe concentration of 0.23 mg mL^{-1}. The Oleic acid-IOs were quickly internalized into the cells within 24 h, with an uptake of 163 pg Fe $cell^{-1}$. The amount taken in by the cells decreased with time because of the rapid growth and division of the macrophage cells. After grafting with PEO, the SCL-P@IO nanoparticles' uptake by macrophage cells was much lower, at only 3 pg Fe $cell^{-1}$, compared with Oleic acid-IO nanoparticles. The very low uptake of SCL-P@IO nanoparticles could be due to surface PEO grafting of the SCL-P@IO nanoparticles lowering the adsorption of the proteins and decreasing the possibility of macrophage recognition.

3.5 Stability test

The stability of the SCL-P@IO nanoparticles under physiological conditions was also studied by DLS measurements. The size change of the SCL-P@IO nanoparticles with incubation time in phosphate-buffered saline (PBS) plus 10% FBS were monitored. As shown in Fig. 5a, the sizes of SCL-P@IO nanoparticles were almost constant over 90 d incubation, indicating that these nanoparticles did not aggregate and were fairly dispersed in the physiological medium. This is mainly attributed to the anti-aggregation and anti-biofouling properties of the PEO blocks of PF127 on the surfaces of SCL-P@IO nanoparticles. The stability of micelles under dilution is also a big issue because they are highly diluted *in vivo* after administration. Pyrene is an effective fluorescent probe to test micelle stability. The ratio between the first (375 nm) and third (386 nm) emission intensities (I_{m1}/I_{m3}) of the pyrene spectrum depends on the environmental polarity of the solvent.[27] Here, the fluorescence spectra of pyrene molecules encapsulated in silica-cross-linked PF127 micelles were measured as a function of PF127 surfactant concentration (different dilution levels) to study the micelle stability. As shown in Fig. 5b, the low and almost constant I_{m1}/I_{m3} ratio (about 1.2 : 1) meant that the silica deposition effectively cross-linked the PF127 micellar chains and stabilized the micelles from dissociation under dilution.

4. Conclusions

In conclusion, we have fabricated a new family of magnetic nanoparticles based on silica cross-linked PF127 block copolymer micelles loaded onto IO nanoparticles. The advantages of high biocompatibility, physical and chemical stability, high magnetism, and the low-cost of production of these new magnetic nanoparticles make them promising for a wide range of biomedical applications, such as bioimaging, bioseparation and drug delivery.

Acknowledgements

This work was supported by the Singapore MOE's ARF Tier 1 funding WBS R-284-000-050-133.

References

1 L. J. D. Thorek, A. K. Chen, J. Czupryna and A. Tsourkas, *Ann. Biomed. Eng.*, 2006, **34**, 23.
2 C. C. Berry and A. S. G. Curtis, *J. Phys. D: Appl. Phys.*, 2003, **36**, R198.
3 A. Ito, M. Shinkai, H. Honda and T. Kobayashi, *J. Biosci. Bioeng.*, 2005, **100**, 1.
4 Y. R. Chemla, H. L. Crossman and Y. Poon, *Proc. Natl. Acad. Sci. U. S. A.*, 2000, **97**, 14268.
5 S. Mornet, S. Vasseur, F. Grasset, P. Veverka, G. Goglio and A. Demourgues, *Prog. Solid State Chem.*, 2006, **34**, 237.

6 L. Yu, Y. Yin, B. T. Mayers and Y. Xia, *Nano Lett*., 2002, **2**, 183.
7 Y. Sahoo, A. Goodarzi, M. T. Swihart, T. Y. Ohulchamskyy, E. P. Furlani and P. N. Prasad, *J. Phys. Chem. B*, 2005, **109**, 3879.
8 H. Lee, E. Lee, D. K. Kim, Y. Y. Heong and S. Jon, *J. Am. Chem. Soc*., 2006, **128**, 7383.
9 L. M. Lacava, Z. G. M. Lacava, M. F. Da Silva, O. Silva, S. S. Chaves, R. B. Azevedo, F. Pelegrini, C. Gansau, N. Buske and P. C. Morais, *Biophys. J*., 2001, **80**, 2483.
10 H. Y. Fan, E. W. Leve, C. Scullin, J. Gabaldon, D. Tallant, S. Bungo, T. Boyle, M. C. Wilson and C. J. Brinker, *Nano Lett*., 2005, **5**, 645.
11 E. Strable, J. W. M. Bulte, B. Moskowitz, K. Vivekanandan, M. Allen and T. Donglas, *Chem. Mater*., 2001, **13**, 2201.
12 N. Kohler, C. Sun, A. Fichtenholtz, J. Gunn, C. Feng and M. Q. Zhang, *Small*, 2006, **2**, 785.
13 F. Quaglia, L. Ostacolo, G. De Rosa, R. La, I. Maria, M. Ammendola, G. Nese, G. Maglio, R. Palumbo and C. Vauthier, *Int. J. Pharm*., 2006, **324**, 56.
14 A. K. Gupta and M. Gupta, *Biomaterials*, 2005, **26**, 3995.
15 P. Wunderbaldinger, L. Josephson and R. Weissleder, *Acad. Radiol*., 2002, **9**, S304.
16 A. Moore, E. Marecos, A. Bogdanov and R. Weissleder, *Radiology*, 2000, **214**, 568.
17 L. Josephson, C. H. Tung, A. Moore and R. Weissleder, *Bioconjugate Chem*., 1999, **10**, 186.
18 H. Choi, S. R. Choi, R. Zhou, H. F. Kung and I. W. Chen, *Acad. Radiol*., 2004, **11**, 996.
19 A. Tsourkas, V. R. Shinde-Patil, K. A. Kelly, P. Patel, A. Wolley, J. R. Allport and R. Weissleder, *Bioconjugate Chem*., 2005, **16**, 576.
20 S. M. Shishido, A. B. Seabra, W. Loh and M. G. de Oliveira, *Biomaterials*, 2003, **24**, 3543.
21 Z. Y. Liu, G. S. Yi, H. T. Zhang, J. Ding, Y. W. Zhang and J. M. Xue, *Chem. Commun*., 2008, **6**, 694.
22 P. D. Yang, D. Y. Zhao, D. I. Margolese, B. F. Chmelka and G. D. Stucky, *Nature*, 1998, **396**, 152.
23 S. H. Sun and H. Zeng, *J. Am. Chem. Soc*., 2002, **24**, 8204.
24 F. Pal, K. Viktoria, L. Karoly, M. Istvan and B. N. Janos, *Microporous Mesoporous Mater*., 2008, **112**, 377.
25 Y. M. Lam, N. Grigorieff and G. Goldbeck-Wood, *Phys. Chem. Chem. Phys*., 1999, **1**, 3331.
26 Z. Y. Liu, X. Quan, H. B. Fu, X. Y. Li and K. Yang, *Appl. Catal., B*, 2004, **52**, 33.
27 E. S. Lee, K. T. Oh, D. Kim, Y. S. Youn and Y. H. Bae, *J. Controlled Release*, 2007, **123**, 19–26.

